DOI: 10.21062/mft.2022.068 http://www.journalmt.com

Research of the Quenched Crankshaft Fatigue Property Based on the Combined Critical Distance and Numerical Simulation Method

Chang Wu (0000-0003-2618-295X)[1], Songsong Sun (0000-0003-1033-2028)[2,*]
College of Automobile and Traffic Engineering, Nanjing Forestry University, Nanjing Jiangsu, 210037, China
*Email: songtang1zhao@163.com

Nowadays the electromagnetic induction quenching approach has been widely applied in the surface treatment process, especially for the parts made by metal materials such as the crankshafts. In this paper, quantitative study was adopted in researching the strengthening effect of this technique. First the multi-physics simulation was achieved to carry out the key information caused by this approach such as the temperature and residual stress distribution property. Then the directly defined critical distance model introduced by Taylor D was combined with the simulation results for the fatigue load prediction. Finally the prediction results were verified according by the standard bending fatigue experiments. The main conclusion of this paper is that the combined critical point method and the Goodmen mean stress model shows the best performance in the prediction. Moreover, the Gerbera mean stress model is the most suitable choice for the critical line method.

Keywords: critical distance, electromagnetic induction quenching, crankshaft, bending fatigue.

1 Introduction

At present, the turbo charging approach has been widely used in automobile engines, which can improve the power and efficiency of the system obviously. As a result of this, more critical strength demand is necessary for the parts which are applied in transferring the power [1-2]. For the engine parts made by iron and steel such as the crankshafts, the electromagnetic induction quenching approach is frequently applied in improving the strength [3-4]. Therefore, essential comprehensive evaluation of the strengthening effect result of this approach must be provided for the generalization.

In recent years, some experts proposed corresponding research in this field. Among these Galunin conducted the finite element simulation process on a wheel gear based on a 3D model, then corresponding shape optimization of the induction coil was accomplished [5]. Sabeeh also researched this problem and discovered that the property design of the process parameters such as the frequency, the power of the coil can create better temperature gradient and temperature distribution in gear, which is benefit to the generation of the harden layer [6]. Stephanie compared the conventional heat treatment techniques with the electromagnetic induction quenching approach and discovered that the mechanical property was affected by the parameters, and the size effect also influenced the strengthening results obviously [7]. Wen chose the internal gear rings to be the research object and conducted the mobile induction approach on it by taking the coil movement factor into account, in this way the key parameter which influenced the quenching results most obviously can be determined. The conclusion of the study can help to design the manufacturing procedure more reasonable [8]. Tong researched the electromagnetic induction quenching approach based on the 3D finite element analysis. The results of the simulation is in keeping with the experimental results. In addition, the key technological parameters during the cooling process could be optimized to improve the mechanical property of the layer [9-10]. Umberto also focused on researching the mechanical property of the layer generated by the electromagnetic induction quenching and determined the key parameters of the approach [11]. Akramchose the EN8 steel to be the object of study and proposed several standard experiments to check the fatigue and wear resistance property of the material after electromagnetic induction quenching. The results showed that the compressive residual stress can obviously improve these mechanical properties, as well as the mircohardness [12].

In previous study, we applied some commonly used mean stress models in researching several types of steel crankshafts after quenching. The theoretical basis of these papers is that the residual stress caused by the manufacturing procedure is just the mean stress [13-14]. The results showed that the predictions based these mean stress models may results in some error in some occasions. The phenomenon may be explained by the differences between the stress and strain states of the part caused by different sources. For this kind of parts with complicated shapes, the stress and strain condition always shows the property of multi-axial no matter what type of load is applied on it.

At present, the critical distance approach has been widely applied in researching the multi-axial problems [15-16]. Compared with the stress or strain models based on the critical plane method, this model has the uniform expression for the application in all kinds of materials, which is benefit for the popularization. So in this paper, the critical distance model proposed by Taylor D was adopted in researching the fatigue property of a type of steel crankshaft. During the research, the mean stress is calculated based on the residual stress distribution along the crack propagation path and the critical distance. The results showed that for the critical point method proposed by Taylor D, the Goodmen mean stress model shows the best performance in the predictions. Moreover, the Gerbera mean stress model is the most suitable choice for the critical line method.

Tab. 1 *Nomenclature*

L	the critical distance
ΔK_{th}	the threshold value of the crack opening stress intensity factor
σ_b	the fatigue strength of the material
$\sigma_{eq}(PM)$	the effective stress according to the critical point method
$\sigma_{eq}(LM)$	the effective stress according to the critical line method
M_a	the applied bending moment load on the crankshaft
M_e	the prediction of the fatigue limit load
h	the equivalent heat transfer coefficient
λ	the thermal conductivity
T_s	the temperature of the crankshaft surface
T_f	the temperature of the crankshaft surface

2 Method

2.1 Research object and material property

In this paper, a type of steel crankshaft applied in heavy trucks was selected as a research object. The material of this crankshaft is 42CrMo. The main components of this material is shown in Table 2, which includes some other metallic elements besides iron and carbon.

Tab. 2 *The main components of the material*

Composition	Percentage/%
C	0.38-0.45
Si	0.17-0.37
Mn	0.50-0.80
S	≤0.035
P	≤0.035
Cr	0.9-1.2
Ni	≤0.3
Cu	≤0.3
Mo	0.15-0.25

During the quenching process, high temperature field will appear at the surface of the steel crankshaft. According to previous study, some parameters of the material property will be influenced by the condition temperature, the relationships between them and the temperature can be found in reference [14].

2.2 Critical distance application method

The critical distance model was a type of typical non-local damage model [17-18]. According to the definition, the fatigue life of a notched component rests with the stress distribution property within its stress concentration area. Then Taylor D proposed an improved model definition method at the beginning of this century, according to which the critical distance can be defined as [19-20]:

$$L = \frac{1}{\pi}\left(\frac{\Delta K_{th}}{\sigma_b}\right)^2 \tag{1}$$

As shown in equation (1), the definitions of the parameters can be found in the nomenclature part. For the commonly used high strength alloy steels, these parameters are easy to find according to the fatigue analysis software Femfat. For the critical point, the definition of the effective stress is:

$$\sigma_{eq}(PM) = \sigma\left(r = \frac{L}{2}\right) \tag{2}$$

For the critical line method, corresponding definition can be expressed as:

$$\sigma_{eq}(LM) = \frac{1}{2L}\int_0^{2L} \sigma(r)dr \tag{3}$$

2.3 Prediction method

According to the theory of critical distance, for a notched component, the key parameter in determining its fatigue life is the stress distribution

function within the stress concentration area [21]. So for the quenched steel crankshaft, the combination of the two parameters will affect its fatigue property: the residual stress distribution property that generated within the quenching process, and the alternating stress distribution property under the cyclical load applied on it. As a result of this, it's possible to predict the fatigue limit load of this crankshaft step by step as followed:

Step 1: The magnetic-thermal coupling phenomenon during the quenching process is simulated by a finite element model, which can provide the necessary information for the analysis in the next step.

Step 2: The thermal-mechanical coupling analysis during the air cooling process is also established based on the same finite element model, then the residual stress field generated after quenching is carried out subsequently.

Step 3: The critical distance is calculated according to the definition, then the effective compressive stress caused by the residual stress field within the given range is computed based on the residual stress field and the selected mean stress model.

Step 4: A known bending moment is applied on the crankshaft. Then the prediction is proposed based on the limit effective stress calculated according to the strengthening factor obtained in the previous step and the effective stress calculated based on the same critical distance range. The result can be expressed as:

$$M_e = \frac{\sigma_{eq}(M)}{\sigma_{eq}(A)} \times M_A \tag{4}$$

As shown in equation (4), the definition of the parameters are also included in the nomenclature part. The whole process of the prediction is shown in Figure 1.

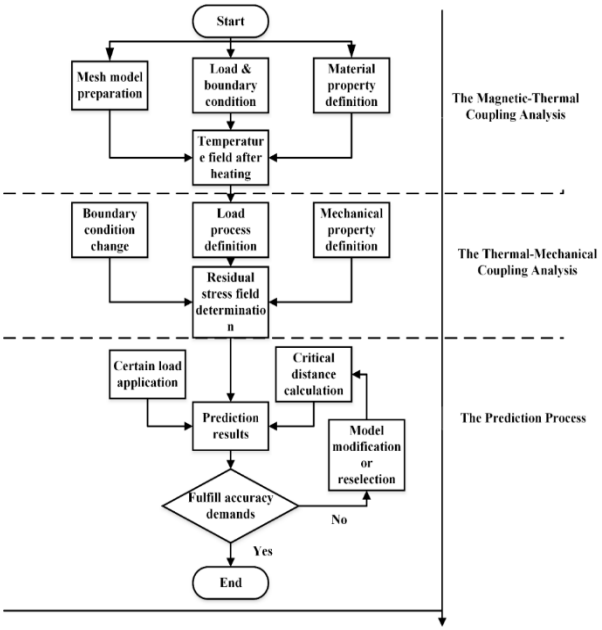

Fig. 1 *The research method of the paper*

3 Result and discussion

3.1 The magnetic-thermal coupling analysis

As mentioned in the previous chapter, the temperature field evolutionary process is the indispensable factor in the researching process. At present, this information is usually acquired through numerical simulation methods. Figure 2 shows the finite element model for the magnetic-thermal coupling analysis during the quenching process, according to previous study, the crankpin and the coil around it are approximately axial symmetry. So in this paper, the model was built according to the 2D structural features to reduce the computation amount on the platform from the professional finite element analysis software workbench [22].

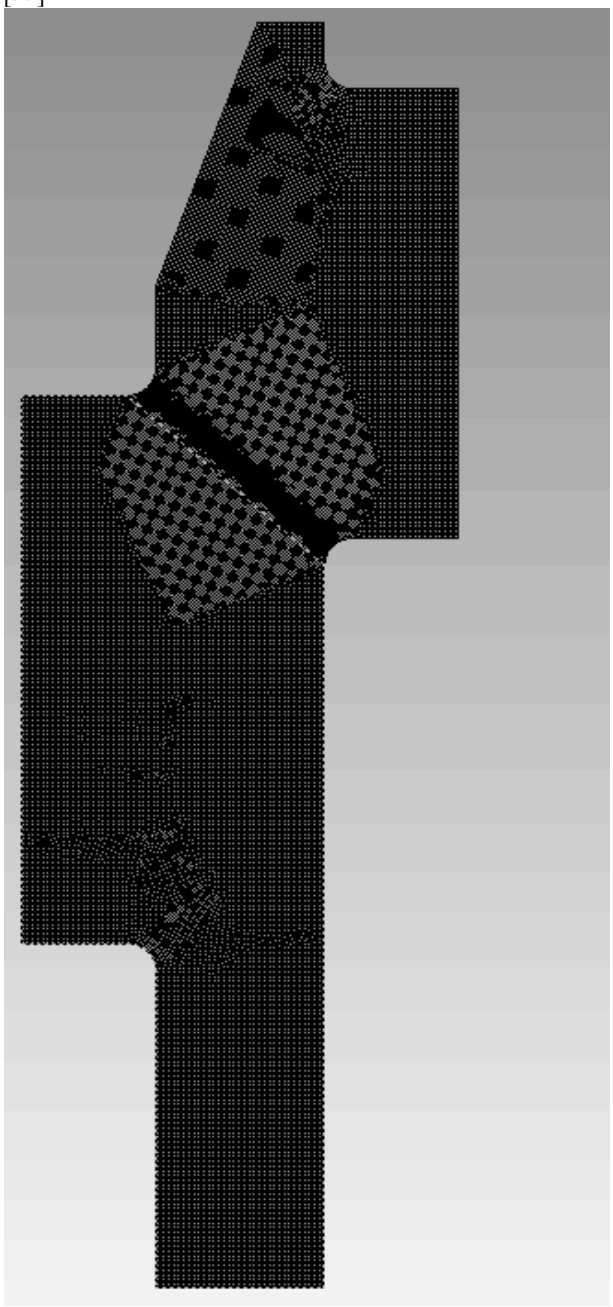

Fig. 2 *The 2D simplified model for the analysis*

During the heating stage of the manufacturing procedure, the alternating current comes through the induction coil and result in the alternating magnetic field which has the same frequency with the current, as well as the heat transfer between the solid metal part and the air. The main types of the heat transfer in this stage are convective and radiative. For the formal type, the thermal boundary condition is defined as [23]:

$$-\lambda \frac{\partial T}{\partial n} = h(T_S - T_f) \tag{5}$$

As shown in equation (5), the detailed definitions of the parameters are introduced in the nomenclature. In addition, the load is just the high frequency alternating current inside the coils. In this paper, the density of the current inside the fillet coil is larger than that inside the crankpin coil. Table 3 shows the detailed information of the load and boundary conditions. In this situation, both the temperature and stress fields are generated by the high frequency alternating current within the coils.

Tab. 3 *The load parameters of the quenching process*

Load and Boundary Parameter	Value
Current frequency	8000Hz
Fillet working time	9s
Crankpin working time	3s
Current intensity	350A
Current density (fillet coil)	$9.9 \times 10^7 A/m^2$
Current density (crankpin coil)	$1.15 \times 10^8 A/m^2$

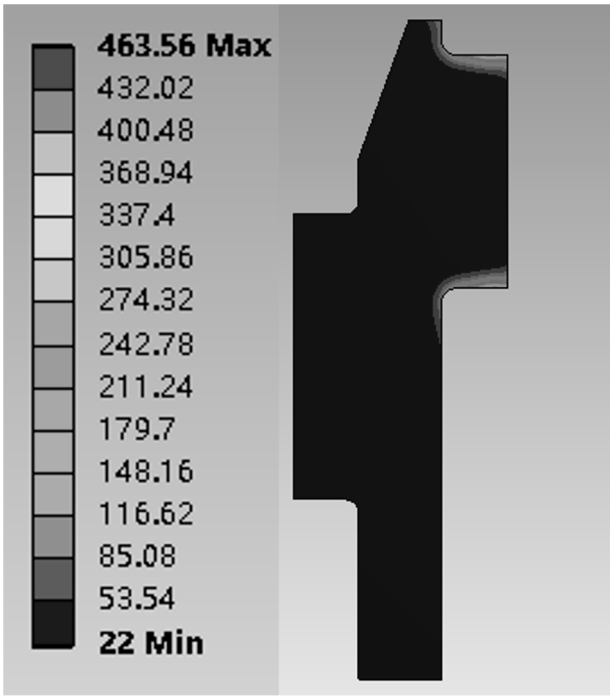

Fig. 3 *The distribution of the temperature (t=3s)*

Based on these information and the mesh model, it's possible to conduct the thermo-mechanical analysis. Figure 3 and Figure 5 shows the temperature field simulation results at different time nodes during the heating stage, it's obvious that with the increase of the heating time, the most obvious increase of the temperature happens at the surface of the crankpin. While for the inner part, the temperature is still nearly the same to the room temperature. The main reason for this difference can be explained by the location of the heat source, because of the skin effect, induced electromotive force and alternating eddy current will be generated within surface area of the steel crankshaft which has been placed in the magnetic field in advance. As a result of this, the growth speed of the temperature within this area is the highest.

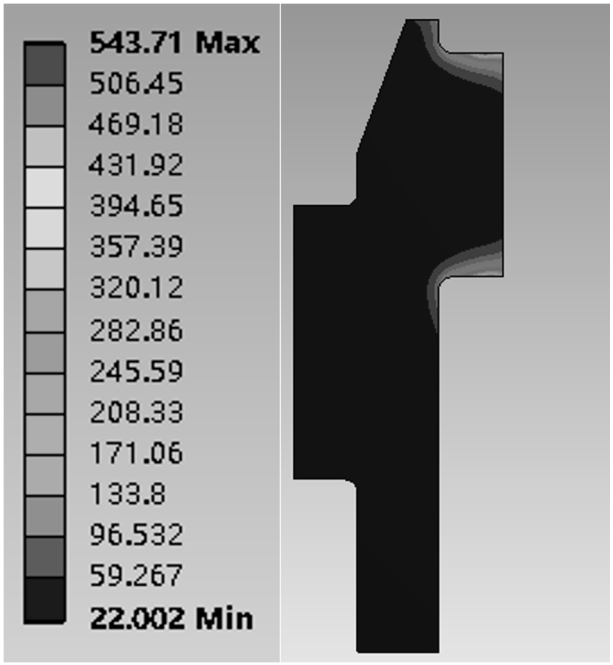

Fig. 4 *The distribution of the temperature (t=6s)*

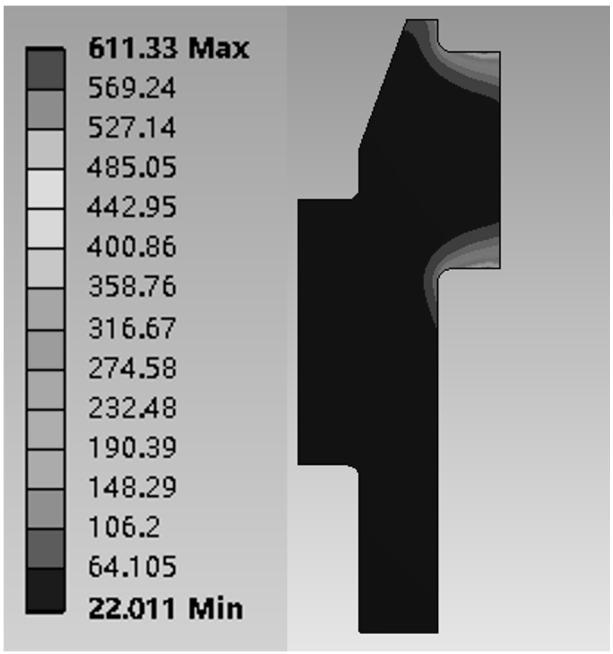

Fig. 5 *The distribution of the temperature (t=9s)*

3.2 The thermal-mechanical coupling

According to the manufacturing procedure, liquid coolant will be spread to the surface of the crankshaft. This will result in the rapid reduction of the surface temperature. Figure 6 shows the temperature field after this operation process, from which it's easy to find that the surface temperature of the whole part is quite near to the room.

As shown in Figure 6, the surface temperature of the crankpin is nearly the same to the room temperature after liquid cooling. While for the central part of the crankshaft, higher temperature appears. After 10 seconds, the highest temperature has reduced to 89°C.

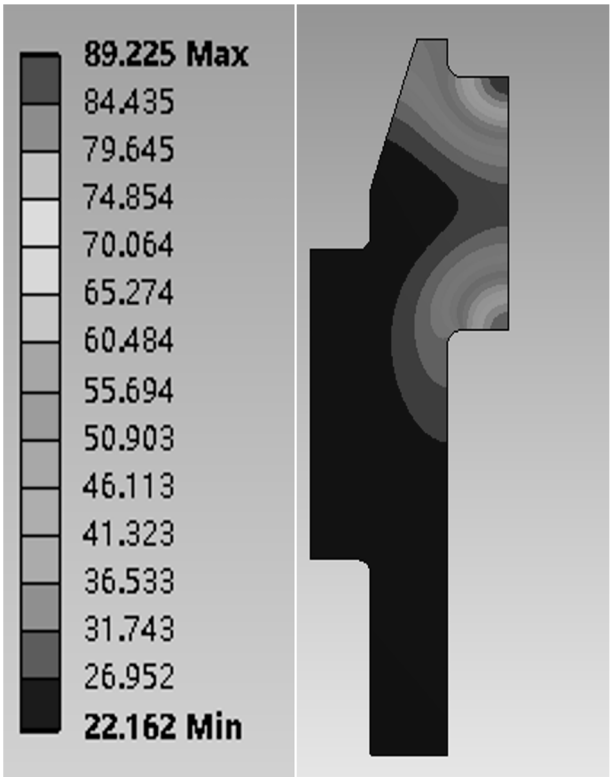

Fig. 6 *The temperature field after liquid cooling*

As shown in Figure 6, for the inner part of the crankshaft, the temperature is still higher than the room temperature. As a result of this, the inner thermal stress caused by the uneven temperature field will result in the final residual stress field [24-25]. This means that the load which generated the residual stress is just the temperature field changing event. In addition, due to the structural symmetry of the crankshaft, the symmetry plane was fixed accordingly. Figure 7 shows the residual stress field analysis result. At the maximum stress point, the residual stress value is 690MPa. While for the fillet point, corresponding value of the stress is 376MPa.

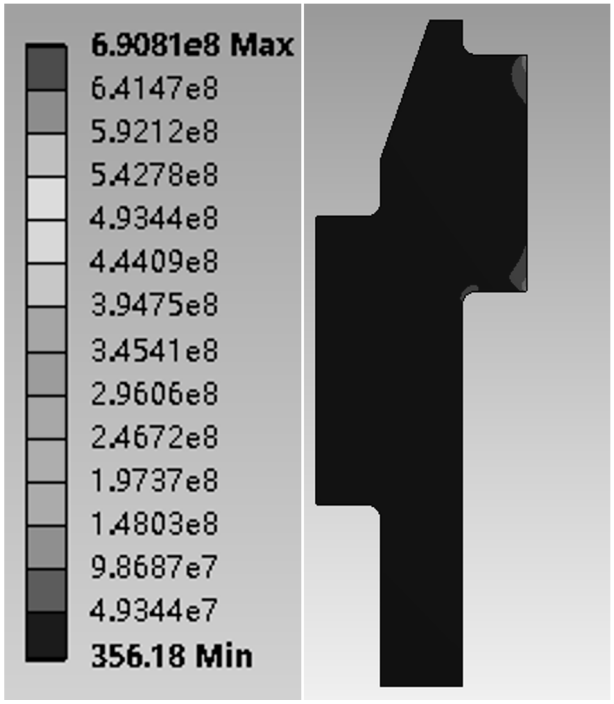

Fig. 7 *The residual stress field of the crankshaft*

3.3 The critical distance calculation

According to the residual stress field distribution property acquired through the simulation process, the strengthening factor can be calculated based on this and the critical distance. According to the material bank of the fatigue analysis software Femfat, the fatigue limit and the threshold value of the crack opening stress intensity factor of the crankshaft material 42CrMo are 396MPa and 21.9MPa·mm$^{0.5}$. So the critical distance according to the directly defined model can be expressed as [26]:

$$L = \frac{1}{\pi}\left(\frac{\Delta K_{th}}{\sigma_b}\right)^2 = 0.56mm \tag{6}$$

Figure 8 shows the fatigue crack path of the crankshaft caused by the bending fatigue experiment, which can be found that the crack initiates from the fillet of the crankpin and spreads to the top left area. According to the critical distance theory, the stress along this line is selected to calculate the effective stress based on different models. The stress of the element nodes on this path is shown in Table 4.

Tab. 4 *The residual stress distribution of crankshaft N0 (along the critical distance direction)*

Distance (mm)	Stress(MPa)
0.2	322
0.4	314
0.6	337
0.8	284
1.0	261
1.2	245
1.4	231
1.6	221

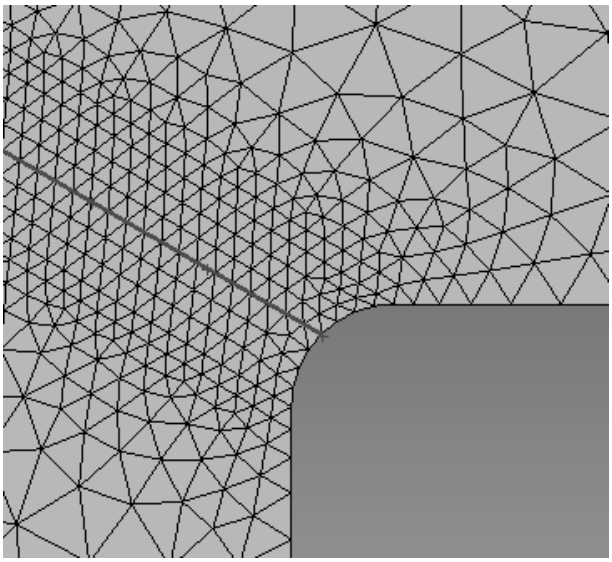

Fig. 8 *The fatigue crack propagation path caused by the bending fatigue test*

Based on these node stress values, it's conveniently to calculate the effective residual stress based on the interpolation method and the critical distance model [27]. The results of the effective mean stress based on different method are shown as followed:

$$\sigma_{eq}(PM) = \sigma(r = 0.28mm) = 317.2MPa \quad (7)$$

$$\sigma_{eq}(LM) = \frac{1}{1.12}\int_0^{1.12} \sigma(r)dr = 307.8MPa \quad (8)$$

3.4 Predictions based on different mean stress models

According to previous research, several mean stress models are usually applied in evaluating the mean stress effect in component fatigue research [13]. Figure 9 shows the S-N curve of the material. Based on the definition and the effective mean stress analysis results above, the limit effective stress calculated according to these mean stress models are shown in Table 5.

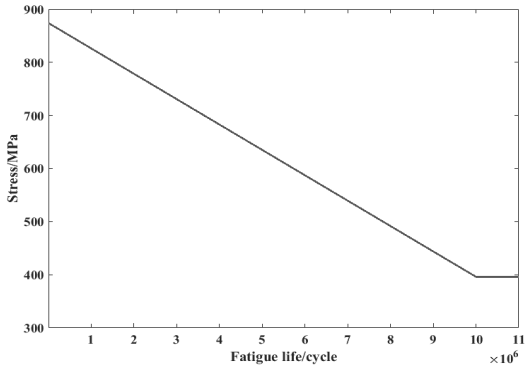

Fig. 9 *The S-N curve of the material*

Tab. 5 *The limit effective stress based on different critical methods and mean stress models*

PM		LM	
Model type	Limit effective stress	Model type	Limit effective stress
Goodman	540MPa	Goodman	536MPa
Gerbera	448 MPa	Gerbera	445MPa

As shown in Table 5, it can be discovered that the values of the limit effective stress obtained by different mean stress models and a given critical distance method (point or line) are quite different from each other. While for a given mean stress model, the limit effective analysis results based on different critical distance methods (point and line) are nearly the same.Figure10 shows the 3D bending fatigue analysis model of the same part, from which it can be discovered that the right face is the load plane and the left face is fixed to provide the basic displacement boundary conditions.

With the combination of this finite element model and the interpolation method, it's convenient to show the stress distribution property of the crankshaft under a given load. Figure 11 shows the stress nephogram of the crankshaft under the given bending moment (1000 $N•m$), from which the maximum stress point can be found at the fillet of the crankpin with the value of 210.8 MPa. The stress distribution of the crankshaft under this load is shown in Table 6.

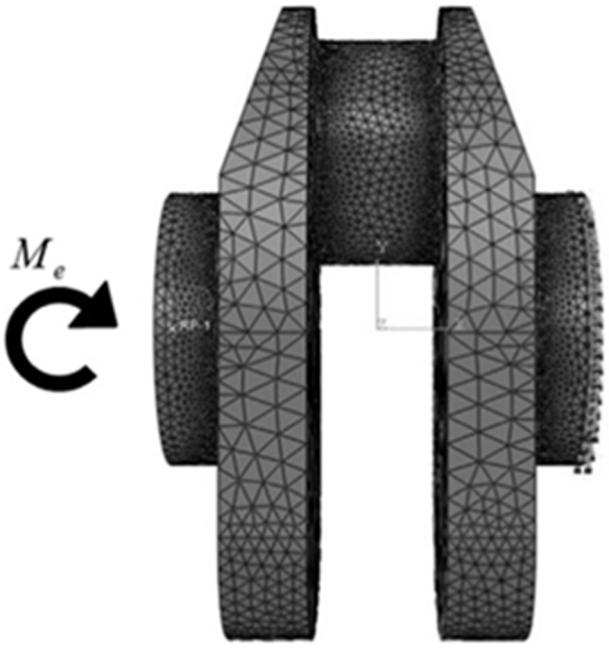

Fig. 10 *The finite element model for bending analysis*

Tab. 6 *The stress distribution of the crankshaft under the given bending moment*

Distance (mm)	Stress(MPa)
0.2	174.35
0.4	143.75
0.6	125.76
0.8	107.87
1.0	96.6
1.2	85.52
1.4	77.77
1.6	70.41

Based on this distribution property and the critical distance value, it's possible to acquire the effective stress in this load condition, corresponding results can be expressed as:

$$\sigma_{eq}(PM) = \sigma(r = 0.28mm) = 160.95MPa \quad (9)$$

$$\sigma_{eq}(LM) = \frac{1}{1.12}\int_0^{1.12} \sigma(r)dr = 135.5MPa \quad (10)$$

By comparing these parameters and the limit effective stress in Table 5, the predictions can be proposed according to equation 4. Corresponding results are shown in Table 7.

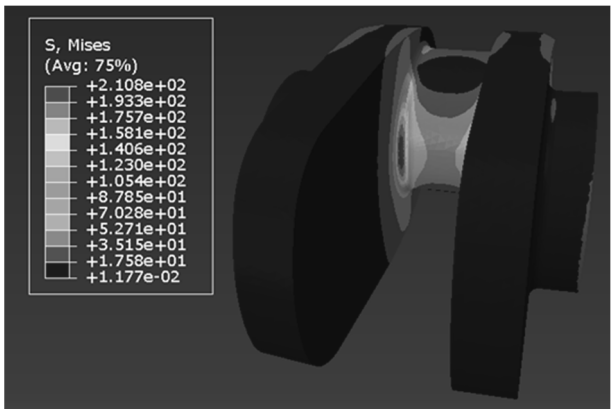

Fig. 11 *The stress nephogram of the crankshaft under the given bending moment*

Tab. 7 *Predictions based on different critical distance methods and mean stress models*

PM		LM	
Model type	Prediction	Model type	Prediction
Goodman	$3355N{\cdot}m$	Goodman	$3956N{\cdot}m$
Gerbera	$2783N{\cdot}m$	Gerbera	$3284N{\cdot}m$

3.5 Experimental verification and discussion

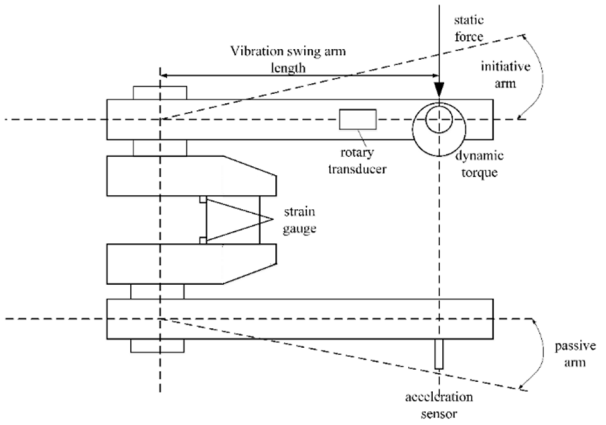

Fig. 12 *The experiment setup for the crankshaft*

As shown in Table 7, the predictions based on these critical distance methods and mean stress models show obvious differences, so corresponding experimental verification is necessary. As shown in Figure 12, the bending fatigue experiment in this paper is operated on this platform. During the fatigue experiment process, a cyclic bending moment generated by the electromotor is applied on the crankshaft to approximately simulate the working condition of the part. As a result of this, the fatigue crack caused by this load will grow from the fillet of the crankpin to reduce the system stiffness. Correspondingly the rotate speed of the electromotor will decline to make the dynamic response of the system unchanged, as well as the effective value of the alternating bending moment. When the reduction of the speed has reached a determined value, the crankshaft is considered broken [28-29]. The detailed results are shown in Table 8.

Tab. 8 *The bending fatigue experimental results of the crankshaft*

Load Value/$N{\cdot}m$	Load Cycle
3335	6,711,179
3436	6,187,261
3881	4,502,460
3941	2,465,780
3941	273,493
3901	548,588
3416	6,142,771
3557	3,509,554

As shown in Table 8, according to the statistical analysis method, the fatigue limit load of the crankshaft is $3335N{\cdot}m$ [30]. The errors of these predictions are displayed in Table 9 in detail. Generally speaking, the accuracy of the predictions are variable within a wide range. For the critical point method, the Goodmen model is more reasonable to be the selection (the error is less than 5%). While for the critical line method, the Gerbera model shows more obvious outstanding performance.

Tab. 9 *Predictionerrors based on different critical distance methods and mean stress models*

PM		LM	
Model type	**Error**	**Model type**	**Error**
Goodman	**0.6%**	**Goodman**	**18.6%**
Gerbera	**16.6%**	**Gerbera**	**1.6%**

From Table 9, it's not difficult to find out that for either mean stress model, the prediction accuracy of different critical distance methods are quite different from each other, although the values of the limit effective stress are nearly the same. One of the primary reasons for this phenomenon is the difference of the types of the stress from different sources along the crack growth path. For the residual stress in this range, the type is gradually converted from compressive to tensile. While for the alternating stress, the type within the range remains unchanged. This difference makes the strengthening effect caused by the effective stress at different point (point or line) not the same.

4 Conclusion

In this paper, a new prediction method was proposed in researching the fatigue property of the quenched steel crankshaft. First, a simplified 2D finite element model was created to analyze the multi-physic coupling reactions during the manufacturing process. Second, the directly defined critical distance model was adopted in analyzing the coupling effect of the stress from different sources during the working period. Finally, the predictions were checked through standard bending fatigue test. The conclusions proposed from this paper is that the prediction method can provide accurate results in keeping with the experimental results in some conditions, but will be influenced by the mean stress model obviously, thus proper combination of the models is necessary to provide the good applicability in actual engineering.

Reference

[1] TIAN, J., TONG, J., & LUO, S. (2018). Differential steering control of four-wheel independent-drive electric vehicles. *Energies*, 11(11): 2892.https://doi.org/10.3390/en11112892

[2] TIAN, J., WANG, Q., DING, J., WANG, Y., & MA, Z. (2019). Integrated Control with DYC and DSS for 4WID Electric Vehicles. *IEEE Access, 7*: 124077-124086. DOI: 10.1109/ACCESS.2019.2937904

[3] GOMES, J., GAIVOTA, N., MARTINS, R. F., & SILVA, P. P. (2018). Failure analysis of crankshafts used in maritime V12 diesel engines. *Engineering Failure Analysis*,92: 466-479.https://doi.org/10.1016/j.engfailanal.2018.06.020

[4] WANG, H., YANG, S., HAN, L., FAN, H., & JIANG, Q. (2020). Failure analysis of crankshaft of fracturing pump. *Engineering Failure Analysis*, 109: 104378.https://doi.org/10.1016/j.engfailanal.2020.104378

[5] GALUNIN, S., KUDRYASH, M., BLINOV, K., &KOZULINA, T. (2015). Numerical simulation and optimization of heater for induction hardening of leading wheel gear. *2015 IEEE NW Russia Young Researchers in Electrical and Electronic Engineering Conference* (EIConRusNW), St. Petersburg, Russia, IEEE,192-195.DOI: 10.1109/EIConRusNW.2015.7102260

[6] SABEEH, H. F., ABDULBAQI, I. M., & MAHDI, S. M. (2018).A 3D FEA Approach to Design an Induction Coil for Case Hardening of a Carbon Steel Gear. *2018 Third Scientific Conference of Electrical Engineering (SCEE)*, Baghdad, Iraq, IEEE, 327-332.DOI: 10.1109/SCEE.2018.8684208

[7] SACKL, S., LEITNER, H., ZUBER, M., CLEMENS, H., & PRIMIG, S. (2014). Induction hardening vs conventional hardening of a heat treatable steel. *Metallurgical and Materials Transactions A*, 45: 5657-5666.https://doi.org/10.1007/s11661-014-2518-4

[8] WEN, H., & HAN, Y. (2017). Study on Mobile Induction Heating Process of Internal Gear Rings for Wind Power Generation. *Applied Thermal Engineering*, 112: 507-515.https://doi.org/10.1016/j.applthermaleng.2016.10.113

[9] TONG, D., GU, J., & YANG, F. (2018).Numerical simulation on induction heat treatment process of a shaft part: Involving induction hardening and tempering. *Journal of Materials Processing Technology*, 262: 277-289. https://doi.org/10.1016/j.jmatprotec.2018.06.043

[10] TONG, D., GU, J., & TOTTEN, G. E. (2018). Numerical investigation of asynchronous dual-frequency induction hardening of spur gear. *International Journal of Mechanical Sciences*, 142-143: 1-9.https://doi.org/10.1016/j.ijmecsci.2018.04.036

[11] PRISCO, U. (2018) Case microstructure in induction surface hardening of steels: An overview. *The International Journal of Advanced Manufacturing Technology*, 98: 2619-2637.https://doi.org/10.1007/s00170-018-2412-0

[12] AKRAM, S., BABUTSKYI, A., CHRYSANTHOU, A., MONTALVÃO, D., WHITING, M. J., & MODI, O. P. (2021). Improvement of the wear resistance of EN8steel by application of alternating magnetic field treatment. *Wear*, 484-485: 203926.https://doi.org/10.1016/j.wear.2021.203926

[13] WU, C., & SUN, S. (2021). Crankshaft High Cycle Bending Fatigue Research Based on a 2D Simplified Model and Different Mean Stress Models. *Journal of Failure Analysis and Prevention*, 21: 1396-1402.https://doi.org/10.1007/s11668-021-01192-w

[14] SUN, S.S., ZHANG, X., WU, C., WAN, M., ZHAO, F. (2021). Crankshaft high cycle bending fatigue research based on the simulation of electromagnetic induction quenching and the mean stress effect. *Engineering Failure Analysis*, 122: 105214.https://doi.org/10.1016/j.engfailanal.2021.105214

[15] TAYLOR, D. (2008). The theory of critical distances. *Engineering Fracture Mechanics*,75: 1696-1705.https://doi.org/10.1016/j.engfracmech.2007.04.007

[16] TAYLOR, D. (2011). Applications of the theory of critical distances in failure analysis. *Engineering Failure Analysis*, 18(2): 543-549.https://doi.org/10.1016/j.engfailanal.2010.07.002

[17] NEUBER, H. (1958).Theory of Notch Stresses: Principles for Exact Calculation of Strength With Reference to Structural Form and Material, 2nd ed, Springer Verlag, Berlin.

[18] PETERSON, R.E. (1959).Notch sensitivity, in: G. Sines, J.L. Waisman (Eds.), Metal Fatigue, McGraw Hill, New York,293–306.

[19] TAYLOR, D., BOLOGNA, P., & KNANI, K. B. (2000). Prediction of fatigue failure location on a component using a critical distance method. *International Journal of Fatigue*, 22(9): 735-742.https://doi.org/10.1016/S0142-1123(00)00062-1

[20] KASIRI, S., & TAYLOR, D. (2008). A critical distance study of stress concentrations in bone. *Journal of Biomechanics*, 41(3): 603-609.https://doi.org/10.1016/j.jbiomech.2007.10.003

[21] SALVETR, P., NOVÝ, Z., GOKHMAN, A., KOTOUS, J., ZMEKO, J., MOTYČKA, P., DLOUHÝ, J. (2020).Influence of Si and Cu content on tempering and properties of 54SiCr6 steel. *Manufacturing Technology*, 20(4):516-520. DOI: 10.21062/mft.2020.079

[22] HE, J., WANG, K., & LI, J. (2021).Numerical Analysis of the Convective Heat Transfer Coefficient Enhancement of a Pyro-Breaker Utilized in Superconducting Fusion Facilities. *Energies*,14(22): 7565.https://doi.org/10.3390/en14227565

[23] SUN, S., GONG, X., & XU, X. (2022).Research on the Bending Fatigue Property of Quenched Crankshaft Based on the Multi-Physics Coupling Numerical Simulation Approaches and the KBM Model. *Metals*, 12(6): 1007.https://doi.org/10.3390/met12061007

[24] JENÍČEK, Š., OPATOVÁ, K., HAJŠMAN, J., & VOREL, I. (2022). Evolution of Mechanical Properties and Microstructure in Q&P Processed Unconventional Medium-Carbon Silicon Steel and Comparison between Q&P Processing, Quenching and Tempering, and Austemperingfor. *Manufacturing Technology*, 22(2), 146-155. DOI: 10.21062/mft.2022.026

[25] HAN, P., & WANG, X. (2021). The Mechanical Performance Evaluation of Vertical Stability Coil under Electro-magnetic-structure Coupling Analyses. *Manufacturing Technology*, 21(1), 65-70. DOI: 10.21062/mft.2021.016

[26] SUN, S.S., WAN, M.S., WANG, H., ZHANG, Y., XU, X.M. (2019). Study of component high cycle bending fatigue based on a new critical distance approach. *Engineering Failure Analysis*, 102: 395-406,.https://doi.org/10.1016/j.engfailanal.2019.04.050

[27] SUN, S. S., YU, X. L., CHEN, X. P., & LIU, Z. T. (2016). Component structural equivalent research based on different failure strength criterions and the theory of critical distance. *Engineering Failure Analysis*, 70: 31–43.https://doi.org/10.1016/j.engfailanal.2016.07.005

[28] ZHOU, X., YU, X. (2007). Failure criterion in resonant bending fatigue test for crankshafts. *Chinese Internal Combustion Engine Engineering*, 28(5): 45-47.

[29] ZHOU, X., YU, X. (2007). Error analysis and load calibration technique investigation of resonant loading fatigue test for crankshaft. *Transactions of the Chinese Society for Agricultural Machinery*, (4): 35-38.

[30] CHEN, X., YU, X., HU, R., & LI, J. (2014). Statistical distribution of crankshaft fatigue: Experiment and modeling. *Engineering Failure Analysis*, 42: 210–220.https://doi.org/10.1016/j.engfailanal.2014.04.015